Structural basis for recruitment of tandem hotdog domains in acyl-CoA thioesterase 7 and its role in inflammation

Jade K. Forwood*[†‡], Anil S. Thakur*, Gregor Guncar*[§¶], Mary Marfori*, Dmitri Mouradov*, Weining Meng*[§], Jodie Robinson[§‖], Thomas Huber*, Stuart Kellie*[§‖], Jennifer L. Martin*[§**], David A. Hume*[§‖**††], and Bostjan Kobe*[‡§**]

*School of Molecular and Microbial Sciences, [§]Institute for Molecular Bioscience, [‖]Cooperative Research Centre for Chronic Inflammatory Diseases, and **Australian Research Council Special Research Centre for Functional and Applied Genomics, University of Queensland, Brisbane, Queensland 4072, Australia

Edited by Gregory A. Petsko, Brandeis University, Waltham, MA, and approved May 10, 2007 (received for review February 2, 2007)

Acyl-CoA thioesterases (Acots) catalyze the hydrolysis of fatty acyl-CoA to free fatty acid and CoA and thereby regulate lipid metabolism and cellular signaling. We present a comprehensive structural and functional characterization of mouse acyl-CoA thioesterase 7 (Acot7). Whereas prokaryotic homologues possess a single thioesterase domain, mammalian Acot7 contains a pair of domains in tandem. We determined the crystal structures of both the N- and C-terminal domains of the mouse enzyme, and inferred the structure of the full-length enzyme using a combination of chemical cross-linking, mass spectrometry, and molecular modeling. The quaternary arrangement in Acot7 features a trimer of hotdog fold dimers. Both domains of Acot7 are required for activity, but only one of two possible active sites in the dimer is functional. Asn-24 and Asp-213 (from N- and C-domains, respectively) were identified as the catalytic residues through site-directed mutagenesis. An enzyme with higher activity than wild-type Acot7 was obtained by mutating the residues in the nonfunctional active site. Recombinant Acot7 was shown to have the highest activity toward arachidonoyl-CoA, suggesting a function in eicosanoid metabolism. In line with the proposal, Acot7 was shown to be highly expressed in macrophages and up-regulated by lipopolysaccharide. Overexpression of Acot7 in a macrophage cell line modified the production of prostaglandins D2 and E2. Together, the results link the molecular and cellular functions of Acot7 and identify the enzyme as a candidate drug target in inflammatory disease.

domain duplication | macrophage | protein structure | acyl-coenzyme A hydrolase | lipid metabolism

Acyl-CoA thioesterases (Acots) catalyze the hydrolysis of fatty acyl-CoA (CoA) ester molecules to CoA and free fatty acid. Acots are therefore able to modulate the cellular levels of activated fatty acids (acyl-CoAs), free fatty acids, and CoA and, in turn, regulate lipid metabolism and other intracellular processes that depend on such molecules (1–3). In higher organisms, different Acot isoforms are localized to distinct cellular organelles including peroxisomes, endoplasmic reticulum, cytosol, and mitochondria (2). Acots cleave a broad range of activated CoA-ester substrates including prostaglandins, acetyl-CoA, bile acids, and branched-chain fatty acids (2, 4, 5) as well as short- and long-chain saturated and unsaturated acyl-CoAs (6–8). The mouse genome contains 12 genes encoding Acots, broadly classified into type I and type II enzymes based on their molecular mass (2). Type I Acots (Acot1–Acot6) are localized to the cytosol (Acot1) (9), mitochondria (Acot2) (10), and peroxisomes (Acot3–Acot6) (11). The larger, oligomeric type II Acots with molecular masses >100 kDa can have different cellular localizations depending on the isoform (12).

The most extensively studied type II Acot is Acot7 (also known as BACH, CTE-II, ACT, ACH1, and BACHa), which is most highly expressed in brain tissue (3). The enzyme has a preference for long-chain acyl-CoA substrates with fatty acid chains of 8–16 carbon atoms (C_8–C_{16}) (7, 13). Acot7 contains a pair of fused thioesterase domains that share ≈30% sequence identity, with each thioesterase domain predicted to have the hotdog fold structure with an α-helix sausage wrapped by a β-sheet bun (14–16).

Here, we present the crystal structures of the N- and C-terminal thioesterase domains (N- and C-domains) of mouse Acot7, refined at 1.8 and 2.4 Å resolution, respectively. We also present a model of the structure of the full-length enzyme based on distance constraints obtained by mass spectrometric analysis of chemical cross-links (17). We show that both thioesterase domains are required for activity but that only one of two potential active sites is functional and identify the active site residues through mutagenesis.

The cellular function of Acot7 is not well understood. A gross deficiency of the enzyme in the hippocampus of patients with mesial temporal lobe epilepsy points to a role in the brain (18). Activation of transcription of the gene by sterol regulatory element-binding protein 2 suggests a function in cholesterol metabolism (19). To link the structural information with a function, we examined the substrate specificity of recombinant enzyme in detail. Acot7 has high specificity for arachidonoyl-CoA, an important precursor molecule for proinflammatory eicosanoids. We also show that the *Acot7* gene is highly expressed in macrophages and up-regulated by lipopolysaccharide and that overexpression of Acot7 in a macrophage cell line alters the production of prostaglandins D2 and E2. These results suggest a role in eicosanoid synthesis and inflammation and may point to its functions in the brain.

Results and Discussion

Crystal Structure of Acot7 N Domain. We separately crystallized and determined the structures of N- and C-domains of Acot7 at 1.8 and

Author contributions: J.K.F., J.L.M., D.A.H., and B.K. designed research; J.K.F., A.S.T., G.G., M.M., D.M., W.M., and J.R. performed research; J.K.F., A.S.T., G.G., M.M., D.M., W.M., J.R., T.H., S.K., J.L.M., D.A.H., and B.K. contributed new reagents/analytic tools; J.K.F., T.H., S.K., J.L.M., D.A.H., and B.K. analyzed data; and J.K.F., J.L.M., D.A.H., and B.K. wrote the paper.

The authors declare no conflict of interest.

This article is a PNAS Direct Submission.

Abbreviations: Acot, acyl-CoA thioesterase; CoA, coenzyme A; C-domain, C-terminal hotdog domain of Acot7; N-domain, N-terminal hotdog domain of Acot7.

Data deposition: The atomic coordinates and structure factors of the crystal structures reported in this paper have been deposited in the Protein Data Bank, www.pdb.org (PDB ID codes 2V1O and 2Q2B).

[†]Present address: School of Biomedical Sciences, Charles Sturt University, Wagga Wagga 2650, Australia.

[‡]To whom correspondence may be addressed. E-mail: b.kobe@uq.edu.au or jforwood@csu.edu.au.

[¶]On leave from Jozef Stefan Institute, Ljubljana, Slovenia.

[††]Present address: Roslin Institute, Roslin BioCentre, Midlothian EH25 9PS, Scotland.

This article contains supporting information online at www.pnas.org/cgi/content/full/0700974104/DC1.

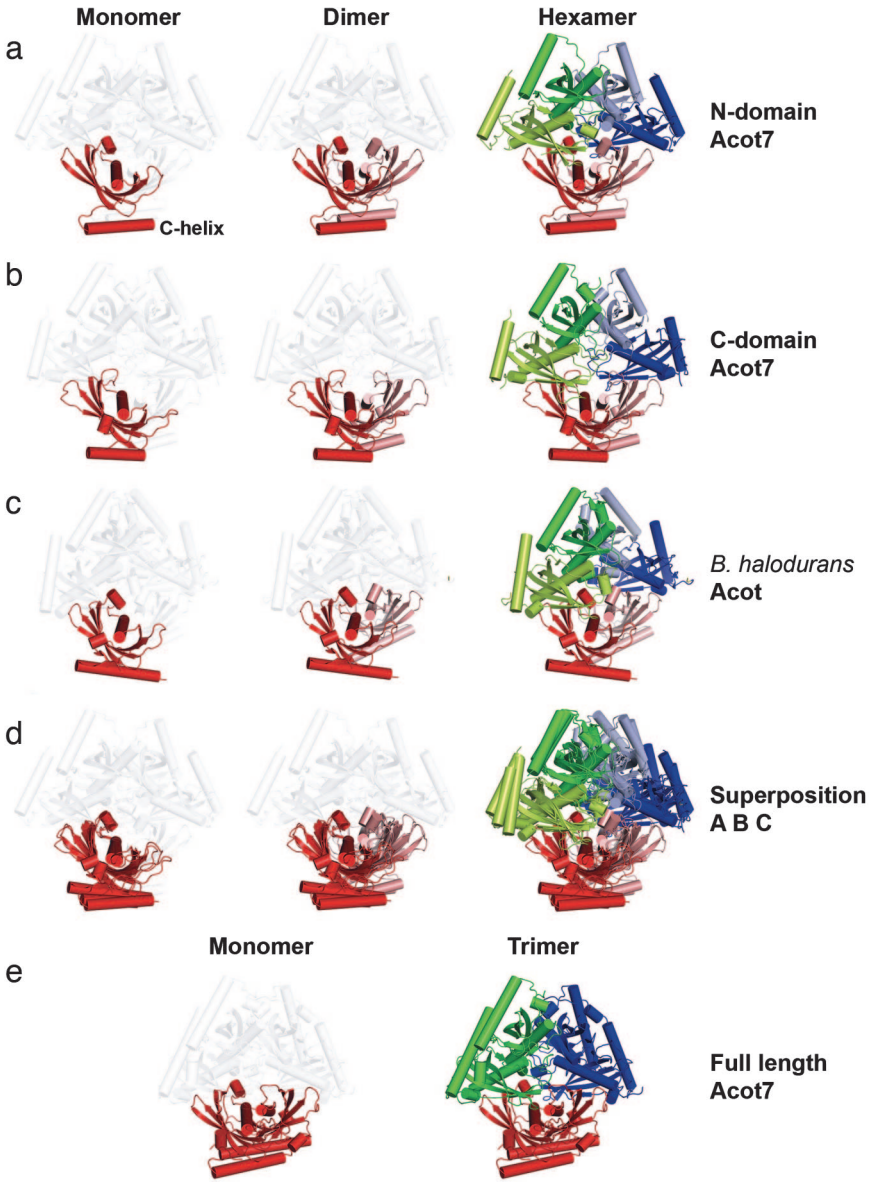

Fig. 1. Structure of Acot7. (*a*) Structure of N-domain of Acot7. The structures are shown in cartoon representation. Each hotdog dimer (protomer) is colored in dark and light shades of the same color. Highlighted are the monomer hotdog domain (*Left*), the protomer (dimer of hotdog domains) (*Center*), and the hexamer (trimer of hotdog dimers) (*Right*). An analogous presentation is used for all of the structures in this figure, and the structures are shown in the same orientation. (*b*) Structure of C-domain of Acot7. (*c*) Structure of the Acot from *B. halodurans* (PDB ID code 1VPM). Rmsd between this structure and (*i*) Acot7 N-domain hexamer is 1.48 Å for 813 Cα atoms; and (*ii*) full-length Acot7 protomer is 2.90 Å for 338 Cα atoms. (*d*) Structural superposition of the Acot7 N-domain, Acot7 C-domain, and *B. halodurans* Acot. (e) Structure of full-length Acot7 showing the monomer and trimer arrangement. All structure diagrams were produced with Pymol (DeLano Scientific LLC) unless stated otherwise. Superimpositions were performed by using CCP4mg (39).

2.5 Å resolution, respectively [supporting information (SI) Table 1]. The N-domain monomer features a five-stranded antiparallel β-sheet surrounding an α-helix (Fig. 1*a*). There is an additional C-terminal α-helix that packs on the opposite side of the β-sheet. Two N-domain monomers associate into a dimer (hereafter referred to as the protomer) displaying a typical double-hotdog structure (20). In the crystals, three protomers further associate into a trimer of protomers. This assembly exists in solution, as determined by size-exclusion chromatography and analytical ultracentrifugation (data not shown).

In the hexamer, the β-sheets form a semicontinuous antiparallel barrel. Approximately 25% of Acot7 residues are involved in interdomain contacts (SI Fig. 5). Six CoA molecules were clearly visible in the electron density, wedged between the two monomers in the protomer (Fig. 2 *a* and *b*). The main interactions with the enzyme include the side chains of Ser-90, His-92, Tyr-152, Lys-156, and Arg-159 from one monomer contacting the phosphates and the 2′-hydroxyl of the 3′-phosphoadenosine diphosphate moiety of CoA, whereas in the neighboring monomer, Asp-69 contacts the amino group of the adenine, and a hydrophobic pocket formed by Val-29, Ile-34, Phe-70, and surrounding residues binds the β-mercapto-ethylamine moiety of CoA. Opposite the CoA-binding site at the domain interface is a large, hydrophobic interdomain tunnel conserved in thioesterases that is likely involved in the fatty-acid chain recognition and release (SI Fig. 6).

Within the Protein Data Bank (PDB), three unpublished structures of bacterial thioesterases (PDB ID codes 1VPM,

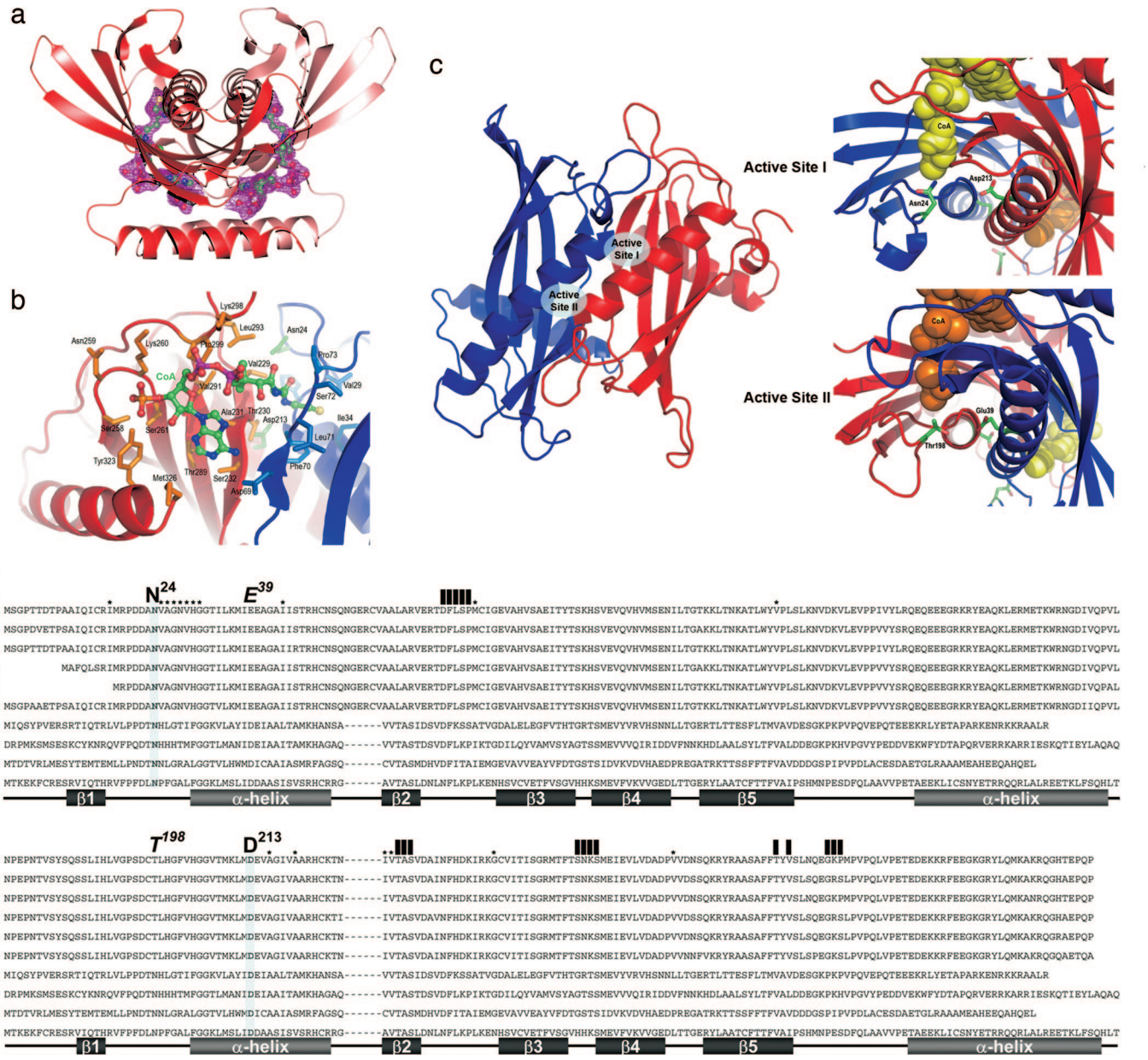

Fig. 2. Acot7 active site. (*a*) Structure of N-domain homodimer, highlighting CoA molecules in ball-and-stick representation. Superimposed is an omit electron density map calculated with coefficients $F_{obs} - F_{calc}$, contoured at 2σ (purple). The diagram was produced by using CCP4mg (39). (*b*) Details of CoA (shown in ball-and-stick representation) binding to N-domain (monomers shown in red and blue in cartoon representation, with the side chains of all residues within 4 Å of CoA in stick representation). (*c*) Structure of full-length Acot7 (in cartoon representation with monomers in red and blue) based on distance constraints derived from chemical cross-linking. Two putative active sites are present within each dual hotdog fold, site I and site II, shown on the right in detail and in an analogous orientation, highlighting CoA (in CPK representation) and the putative catalytic residues (in stick representation). (*d*) Sequence alignment of Acot7 and selected Acots. Prokaryotic homologues contain only a single domain and are aligned to both N- and C-domains of Acot7. Aligned species include (top to bottom): *Mus musculus* (Mm), *Homo sapiens* (Hs), *Rattus norvegicus* (Rn), *Pongo pygmaeus* (Pp), *Canis familiaris* (Cf), *Bos taurus* (Bt), *Tetraodon nigroviridis* (Tn), *Bacillus halodurans* (Bh), *Staphylococcus aureus* (Sa), *Halobacterium sp* (Hs), *Enterococcus faecalis* (Ef). Residues modeled within site I and II are highlighted in bold and bold italics, respectively; CoA-binding residues are highlighted with a vertical black bar, and fatty-acyl-binding residues are highlighted with an asterisk.

1YLI, and 1Y7U) have a similar hexameric arrangement to Acot7, suggesting that this may be common within the family (Fig. 1 *c* and *d*). Other reported oligomeric structures of microbial thioesterases include dimers (20, 21) and different tetrameric arrangements (14, 22, 23).

Crystal Structure of the Acot7 C-domain. The structure of the C-domain is similar to that of the N-domain (rmsd 1.28 Å for 124 Cα atoms in the monomer; 1.60 Å for 248 Cα atoms in the protomer; and 2.26 Å for 744 Cα atoms in the hexamer; Fig. 1*b*). In contrast to the N-domain, the C-domain is a dimer in solution, as determined by size-exclusion chromatography and analytical ultracentrifugation. The area of interaction (876 and 2,017 A^2 surface area buried at the intra- and interprotomer domain interfaces, respectively) is smaller than in the N-terminal domain (1,333 and 3,777 A^2, respectively). CoA was not observed in the crystals despite its inclusion in the crystallization solution.

Acot7 Requires Both Thioesterase Domains for Activity. The functional significance of having two thioesterase domains in Acot7

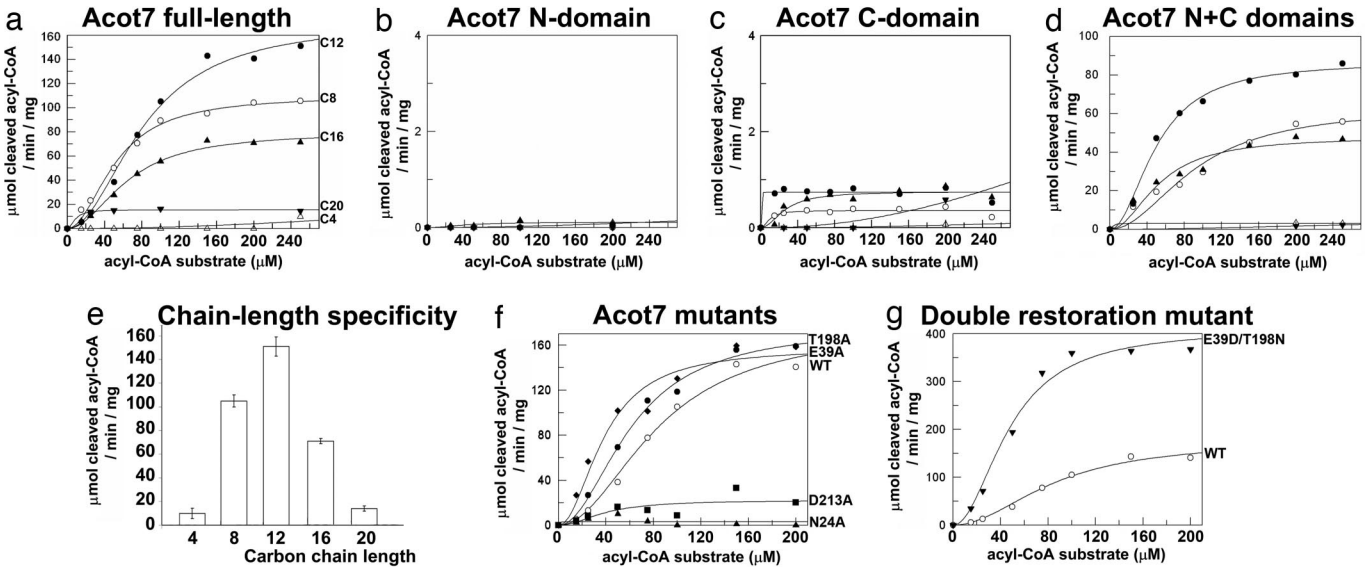

Fig. 3. Enzyme activity and substrate chain length specificity of Acot7. (*a–d*) Activity of full-length Acot7 (*a*); N-domain of Acot7 (*b*); C-domain of Acot7 (*c*); and combined N- and C-domains of Acot 7. (*d*), as a function of the concentration of fatty acyl-CoAs: butyryl (C4:0)-CoA, open triangles; octanoyl (C8:0)-CoA, open circles; lauroyl (C12:0)-CoA, filled circles; palmitoyl (C16:0)-CoA, filled triangles; and arachinoyl (C20:0)-CoA, filled and inverted triangles. (*e*) Profile of chain-length-specificity of full-length Acot7 at a fixed substrate concentration of 200 μM. (*f*) Activity of site I mutants N24A (filled triangles) and D213A (filled squares) and site II mutants E39A (filled diamonds) and T198A (filled circles) against lauroyl (C12:0)-CoA; WT, open circles. (*g*) E39D/T198N double mutant; WT, open circles. The results from a single typical experiment are shown; pooled results are presented in SI Table 2.

and related enzymes has not been studied. The single thioesterase domain from *Bacillus halodurans* forms an active enzyme with highest activity for the short-chain acyl-CoA substrates (J.K.F., M.M., and B.K. unpublished work). To evaluate the functional contributions of each thioesterase domain within Acot7, we compared the catalytic activity (against a range of fatty acyl-CoA substrates) of full-length Acot7 and the individual domains. Full-length Acot7 efficiently hydrolyzed medium- to long-chain (C_8–C_{16}) saturated fatty acyl-CoA substrates, with the maximal activity toward lauroyl-CoA (Fig. 3; SI Table 2). The individual domains had no detectable activity, but when both thioesterase domains of Acot7 were combined, the activity was restored to approximately half that of the wild-type enzyme (Fig. 3). Neither the N- nor C-domain activity of Acot7 could be restored by the thioesterase domain of *B. halodurans* (SI Fig. 7). The results indicate that the N- and C-domains of Acot7 can associate cooperatively to form an active enzyme, whereas homomeric complexes of the N- and C-domains are inactive.

Structure Determination of Full-Length Acot7 by Using Chemical Cross-Linking-Derived Distance Constraints. It has not yet been possible to crystallize full-length Acot7. To gain structural insights into the nature of the cooperation between the N- and C-domains required for catalysis, we performed chemical cross-linking (using two lysine-specific bifunctional cross-linking reagents), followed by MS to identify six interdomain cross-links within Acot7 (SI Table 3). Based on the distance constraints imposed by the length of the cross-linker, we derived a model of Acot7 through docking and molecular modeling (17). The model features the association of the N- and C-domains within a protomer (Fig. 1*e*). The predicted N–C-domain interface (1,787 A^2) is considerably larger than either of the homodimeric N–N or C–C interfaces, and features more interdomain hydrogen bonds (22, 12, and 9 for N–C, N–N, and C–C interfaces, respectively), suggesting a physical basis for the preference of heterodimeric association. The structure is consistent with the trimeric assembly of Acot7 suggested by analytical ultracentrifugation and size-exclusion chromatography.

Intradomain Interfaces Within Acot7 Form Asymmetric Catalytic Active Sites. The trimeric arrangement in Acot7 and the position of CoA molecules in the N-domain suggest that there are three copies each of two distinct potential active sites in Acot7 (Fig. 2*c*). Sequence analysis of CoA-proximal residues in mammalian Acot7s (Fig. 2*d*) suggests that Asn-24 and Asp-213 (forming "site I") are conserved, whereas the analogous residues in site II (Glu-39 and Thr-198) are not conserved. To assess the role of these potential active site residues in catalysis, each residue was mutated to Ala, and the mutant recombinant enzymes were isolated and the activity of the mutant residues characterized (structural integrity of each mutant was verified by circular dichroism and size-exclusion chromatography; data not shown). Both the N24A and D213A mutations resulted in a dramatic reduction in catalytic activity (Fig. 3 and SI Table 4). By contrast, the analogous mutations within site II did not affect activity. The most obvious explanation for this finding is that site II is not involved directly in catalysis. We further constructed the double mutant E39D/T198N, in which the key catalytic residues from site I are introduced into site II; this mutant displayed a 4-fold increase in the catalytic activity compared with wild-type Acot7 (Fig. 3). The results indicate that site I is required for catalysis, whereas site II has a distinct regulatory function. The conversion of site II to an active site not only creates more active sites but relieves an inhibitory activity. Interestingly, the single thioesterase domain of prokaryotic PaaI from *Thermus thermophilus* that contains identical active sites also uses only half of the active sites through an induced-fit mechanism of negative regulation (23). "Half-of-sites" negative regulation has been described in a number of unrelated enzymes including glyceraldehyde 3-phosphate dehydrogenase (24), aspartyl transcarbamylase (25), and pyruvate kinase (26). Negative regulation may place an upper limit on enzymatic efficiency and allow the cell to more precisely regulate the cellular concentrations of its substrates and products.

Acot7 Cleaves Arachidonoyl-CoA and Is Up-Regulated in Activated Macrophages. The available literature on the cellular function of Acot7 is limited. Acot7 is also known as brain acyl-CoA hydro-

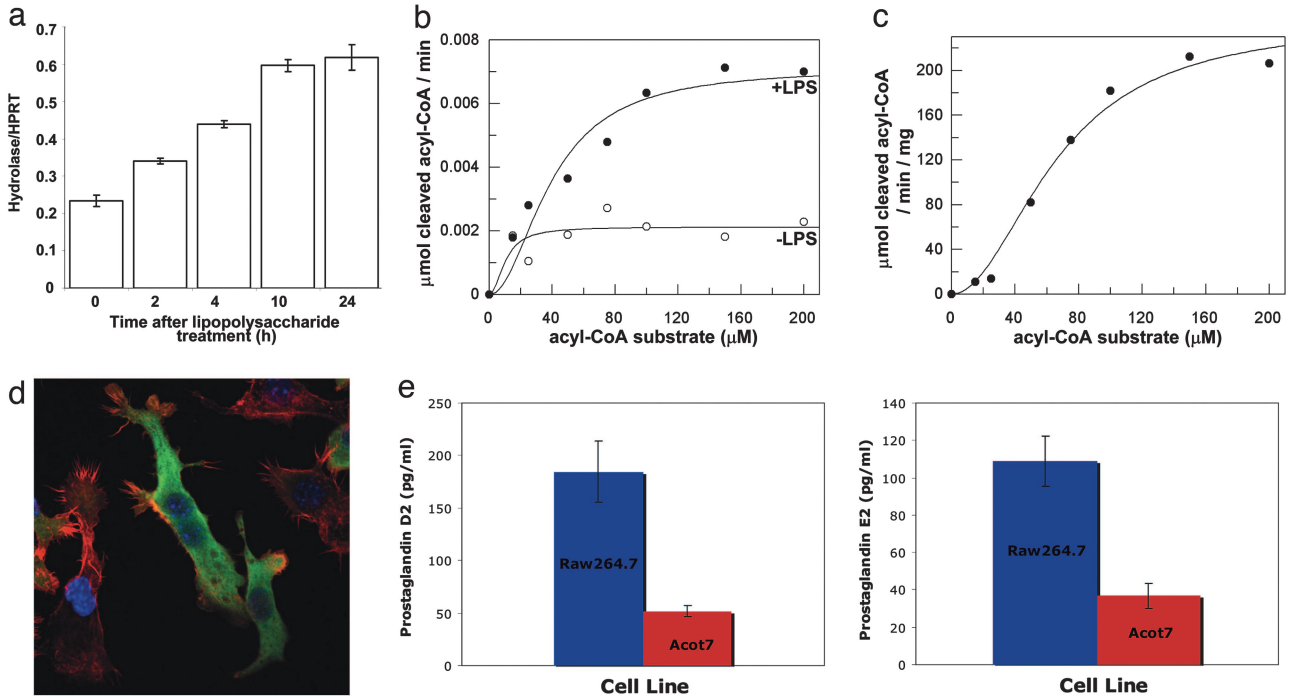

Fig. 4. Acot7 gene expression and acyl-CoA thioesterase activity in macrophage cells. (*a*) Real-time PCR analysis of the Acot7 gene in LPS-induced macrophage cells. (*b*) Thioesterase activity of unstimulated and stimulated macrophage lysates. (*c*) Acot7 thioesterase activity on arachidonoyl-CoA (C20:4-CoA). (*d*) Localization of V5-Acot7 (green) in macrophage cells. Also shown are 4′,6-diamidino-2-phenylindole (DAPI; blue) and phalloidin (red) stains highlighting the nucleus and actin, respectively. (*e*) Prostaglandin levels of D2 and E2 for RAW264.7 (blue) and Acot7-transfected (red) macrophage cells.

lase (BACH) because of its high selective expression in the brain (27, 28). However, microarray profiling (29) and high-throughput analysis of start-site usage by CAGE (30) also demonstrate abundant expression in macrophages and up-regulation by lipopolysaccharide (LPS) and colony-stimulating factor 1 (CSF-1; data accessible through www.macrophages.com). Macrophages provide an experimentally accessible system for functional characterization. To verify the expression data, we carried out quantitative RT-PCR, which confirmed both abundant basal expression and induction of mRNA encoding *Acot7* in mouse macrophages (Fig. 4*a*). These results are supported by an increase in acyl-CoA thioesterase activity for lauroyl-CoA within the lysates of macrophages induced with LPS (Fig. 4*b*).

We considered the possibility that Acot7 expression in macrophages could be associated with the production of lipid-based proinflammatory eiconasoids during an inflammatory response. The precursor for these factors is arachidonic acid, a C_{20} unsaturated fatty-acid containing four cis double bonds. Purified rat Acot7 from brain cytoplasmic extracts (31) and the mitochondrial Acot2 (32–34) were shown previously to hydrolyze arachidonoyl-CoA. Although Acot7 does not efficiently cleave C_{20}-saturated acyl-CoA, arachidonoyl-CoA was more efficiently cleaved by Acot7 than any of the saturated fatty acyl-CoAs tested, suggesting that it is the preferred, and perhaps the important, physiological substrate (Fig. 4*c*).

If Acot7 selectively hydrolyzes arachidonoyl-CoA, overexpression could potentially increase or decrease the release of eicosanoids from activated macrophages. Arachidonoyl-CoA is the precursor of archidonate in the plasma membrane, which is released by phospholipase A2. Acot7 overexpression might deplete the membrane of this eicosanoid precursor. Conversely, Acot7 itself might generate free arachidonic acid from arachidonoyl-CoA, or reduce the pool of arachidonoyl-CoA, which has effector functions in its own right. To test these possibilities, we overexpressed a V5 epitope-tagged Acot7 by transfection of the mouse macrophage cell line, RAW264.7. Immunolocalization indicated a diffuse cytoplasmic location, consistent with its cellular localization in neurons (28) (Fig. 4*d*). Acot7 overexpression strongly suppressed the basal production of prostaglandin D2 and E2; the residual production is likely derived from the subpopulation of cells that do not express the enzyme (Fig. 4*e*). This outcome favors the view that overexpression of Acot7 restricts the incorporation of arachidonic acid into membrane phospholipids. A role in arachidonate metabolism for Acot7 could explain the expression in brain, where arachidonate metabolism contributes to numerous aspects of neuronal function, neuroinflammation, and neurodegeneration (35). The structure and function information in our study indicates that both inhibitors (such as short-chain acyl-CoA) and activators (site II agonists) of enzyme activity are possible. Either could have applications in therapy for inflammatory and neurodegenerative diseases.

Materials and Methods

Cloning, Expression, Purification, Protein Characterization, Mutagenesis, Real-Time PCR, Cell Culture, Subcellular Localization, and Prostaglandin Detection. Standard methods were used as described in *SI Methods*.

Thioesterase Activity Assay. The standard reaction mixture contained the fatty acyl-CoA substrate ranging from 10 to 250 μM, 0.1 μg of protein sample, and 100 mM sodium phosphate (pH 7.4) in a final volume of 1 ml. The absorbance at 232 nm (13) was monitored immediately after adding the substrate and followed for 3 min at 20-s intervals. The molar absorption coefficient, ε_{232} (4,250 $M^{-1}cm^{-1}$) was used to calculate cleavage of the thioester bond (36). GraFit was used to plot the data and calculate maximum velocity and Michaelis–Menten constants.

Crystal Structure Determination. The crystals of C- and N-domains were grown by hanging-drop vapor diffusion in 20% PEG 2000 MME/0.1 M Tris (pH 7.0) (37) and 15% PEG 2000 MME/0.2 M sodium potassium tartrate, respectively. In both cases, initial phases were obtained by molecular replacement by using Phaser (38) and one subunit of the *B. halodurans* acyl-CoA thioesterase (PDB ID 1VPM) as the search model, and the structures were refined by using Refmac (39) and Coot (40). The N- and C-domain models comprise residues 16–161 and 177–326, respectively. The N-domain contains 779 water molecules and six CoA molecules; the C-domain contains 60 water molecules, with residues 194–199 and 276–278 not included in the model because of poor electron density.

Structure Determination of Acot7 by Using Cross-Linking, Distance Constraints, and Molecular Modeling. The procedures and the model are available in *SI Methods*.

We thank Raymond Stevens and the Joint Centre for Structural Genomics for providing the expression construct of *B. halodurans* acyl-CoA thioesterase, and Debra Dunaway-Mariano, Ian Ross, Gordon King, and Lyle Carrington for helpful discussions. We acknowledge the use of the University of Queensland Macromolecular X-ray Crystallography Facility. This work was funded in part by a grant from the Australian Research Council (ARC) (to J.L.M. and B.K.). B.K. is an ARC Federation Fellow and a National Health and Medical Research Council (NHMRC) Honorary Research Fellow. J.L.M. is a NHMRC Research Fellow. J.K.F. was an NHMRC C. J. Martin Fellow.

1. Faergeman NJ, Knudsen J (1997) *Biochem J* 323:1–12.
2. Hunt MC, Alexson SE (2002) *Prog Lipid Res* 41:99–130.
3. Yamada J (2005) *Amino Acids* 28:273–278.
4. Ofman R, el Mrabet L, Dacremont G, Spijer D, Wanders RJ (2002) *Biochem Biophys Res Commun* 290:629–634.
5. Suematsu N, Okamoto K, Isohashi F (2002) *Acta Biochim Pol* 49:937–945.
6. Poupon V, Begue B, Gagnon J, Dautry-Varsat A, Cerf-Bensussan N, Benmerah A (1999) *J Biol Chem* 274:19188–19194.
7. Yamada J, Furihata T, Tamura H, Watanabe T, Suga T (1996) *Arch Biochem Biophys* 326:106–114.
8. Yamada J, Kurata A, Hirata M, Taniguchi T, Takama H, Furihata T, Shiratori K, Iida N, Takagi-Sakuma M, Watanabe T, *et al.* (1999) *J Biochem* 126:1013–1019.
9. Lindquist PJ, Svensson LT, Alexson SE (1998) *Eur J Biochem* 251:631–640.
10. Svensson LT, Engberg ST, Aoyama T, Usuda N, Alexson SE, Hashimoto T (1998) *Biochem J* 329:601–608.
11. Westin MA, Alexson SE, Hunt MC (2004) *J Biol Chem* 279:21841–21848.
12. Hunt MC, Yamada J, Maltais LJ, Wright MW, Podesta EJ, Alexson SE (2005) *J Lipid Res* 46:2029–2032.
13. Yamada J, Matsumoto I, Furihata T, Sakuma M, Suga T (1994) *Arch Biochem Biophys* 308:118–125.
14. Benning MM, Wesenberg G, Liu R, Taylor KL, Dunaway-Mariano D, Holden HM (1998) *J Biol Chem* 273:33572–33579.
15. Dillon SC, Bateman A (2004) *BMC Bioinformatics* 5:109.
16. Leesong M, Henderson BS, Gillig JR, Schwab JM, Smith JL (1996) *Structure (London)*4:253–264.
17. Mouradov D, Craven A, Forwood JK, Flanagan JU, Garcia-Castellanos R, Gomis-Ruth FX, Hume DA, Martin JL, Kobe B, Huber T (2006) *Protein Eng Des Sel* 19:9–16.
18. Yang JW, Czech T, Yamada J, Csaszar E, Baumgartner C, Slavc I, Lubec G (2004) *Amino Acids* 27:269–275.
19. Takagi M, Suto F, Suga T, Yamada J (2005) *Mol Cell Biochem* 275:199–206.
20. Li J, Derewenda U, Dauter Z, Smith S, Derewenda ZS (2000) *Nat Struct Biol* 7:555–559.
21. Hisano T, Tsuge T, Fukui T, Iwata T, Miki K, Doi Y (2003) *J Biol Chem* 278:617–624.
22. Thoden JB, Zhuang Z, Dunaway-Mariano D, Holden HM (2003) *J Biol Chem* 278:43709–43716.
23. Kunishima N, Asada Y, Sugahara M, Ishijima J, Nodake Y, Sugahara M, Miyano M, Kuramitsu S, Yokoyama S, Sugahara M (2005) *J Mol Biol* 352:212–228.
24. Nagradova NK, Kuzminskaya EV, Asryants RA (1993) *Biotechnol Appl Biochem* 18:157–163.
25. Klotz IM, Hunston DL (1977) *Proc Natl Acad Sci USA* 74:4959–4963.
26. Rahmatullah M, Roche TE (1985) *J Biol Chem* 260:10146–10152.
27. Yamada J, Kuramochi Y, Takagi M, Suga T (2004) *Neurosci Lett* 355:89–92.
28. Yamada J, Kuramochi Y, Takagi M, Watanabe T, Suga T (2002) *Biochem Biophys Res Commun* 299:49–56.
29. Wells CA, Ravasi T, Sultana R, Yagi K, Carninci P, Bono H, Faulkner G, Okazaki Y, Quackenbush J, Hume DA, *et al.* (2003) *Genome Res* 13:1360–1365.
30. Carninci P, Sandelin A, Lenhard B, Katayama S, Shimokawa K, Ponjavic J, Semple CA, Taylor MS, Engstrom PG, Frith MC, *et al.* (2006) *Nat Genet* 38:626–635.
31. Broustas CG, Hajra AK (1995) *J Neurochem* 64:2345–2353.
32. Castilla R, Maloberti P, Castillo F, Duarte A, Cano F, Maciel FC, Neuman I, Mendez CF, Paz C, Podesta EJ (2004) *Endocr Res* 30:599–606.
33. Maloberti P, Lozano RC, Mele PG, Cano F, Colonna C, Mendez CF, Paz C, Podesta EJ (2002) *Eur J Biochem* 269:5599–5607.
34. Takagi M, Kawabe K, Suga T, Yamada J (2004) *Arch Biochem Biophys* 429:100–105.
35. Farooqui AA, Ong WY, Horrocks LA (2006) *Pharmacol Rev* 58:591–620.
36. Miyazawa S, Furuta S, Hashimoto T (1981) *Eur J Biochem* 117:425–430.
37. Serek R, Forwood JK, Hume DA, Martin JL, Kobe B (2006) *Acta Crystallogr F* 62:133–135.
38. McCoy AJ, Grosse-Kunstleve RW, Storoni LC, Read RJ (2005) *Acta Crystallogr D* 61:458–464.
39. CCP4 (1994) *Acta Crystallogr D* 50:760–763.
40. Emsley P, Cowtan K (2004) *Acta Crystallogr* D 60, 2126–2132.